IEEE Access
Multidisciplinary | Rapid Review | Open Access Journal

Received 13 May 2025, accepted 13 June 2025, date of publication 20 June 2025, date of current version 27 June 2025.

Digital Object Identifier 10.1109/ACCESS.2025.3581601

APPLIED RESEARCH

Dielectric Lens-Type CATR System Using a Serrated Structure for Antenna Radiation Pattern Measurement

GENMA HATTORI[1,2], (Member, IEEE), SOU EMA[1], YUTA HORIE[1], AND TOSHIYUKI MAEYAMA[2], (Member, IEEE)

[1]Engineering Department, Microwave Factory Company Ltd., Hachioji 193-0985, Japan
[2]Graduate School of Engineering, Takushoku University, Japan

Corresponding author: Genma Hattori (genma.hattori@mwf.co.jp)

ABSTRACT Large aperture antennas are used to compensate for high propagation losses in the millimeter wave bands used by Beyond 5G/6G, satellite, and automotive collision prevention radars. The big anechoic chambers required to accommodate Direct Far-field (DFF) measurements can be prohibitively large and expensive. Establishing anechoic chambers and test ranges large enough to accommodate DFF measurements has proven difficult and costly. More recently, however, the characterization of large aperture millimeter-wave antennas and transceivers can be more economically performed utilizing Compact Antenna Test Range (CATR) systems. Unlike traditional large anechoic chamber-based systems that utilize DFF techniques, CATR systems incorporate Indirect Far-Field (IFF) techniques with reflectors to achieve comparable measurements using less space. This translates into smaller and less expensive test systems. However, conventional reflectors used in millimeter-wave CATR chambers can be expensive to manufacture and set up. This paper proposes a more economical dielectric lens that utilizes a Serrated Structure (SS) around the lens to achieve suitable plane-wave characteristics. The dielectric lens was analyzed using the Finite Element Method (FEM) and then manufactured to theoretical dimensions. As a result, it showed Quiet Zone (QZ) characteristics of 1/3 the diameter of the lens. To show that the manufactured lens could be applied to the CATR system, the results of evaluating the radiation pattern of a 1024-element antenna at 30 GHz are shown below.

INDEX TERMS Antenna, antenna measurement, CATR, lens, plane wave, beyond 5G, 6G, quiet zone, OTA, millimeter wave, serrated structure, lens, reflector.

I. INTRODUCTION

Driven by technological innovation in support of wide bandwidth Beyond 5G/6G applications, antennas in the millimeter wave band are being developed to address unprecedented high-speeds, high-capacity, and low-latency wireless communications [1]. However, to correct for the high propagation loss associated with the millimeter wave bands, a high-gain antenna with a large aperture surface in relation to the wavelength is required [2]. The DFF evaluation conditions of such a high-gain antenna radiation pattern are described in equation (1), with the distance between the transmitting and receiving antennas set accordingly [3]. The minimum distance will be

$$R \geq \frac{2D_1^2}{\lambda} \tag{1}$$

where D_1 is the maximum size of DUT (Device Under Test), and λ is wavelength.

This equation prescribes a state in which the path difference between the center and edge of the antenna satisfies $\lambda/16$, and a phase error of 2% ($\approx$22.5 deg.) maximum. However, this is derived under the condition that one antenna is a point source and the other has an aperture.

The associate editor coordinating the review of this manuscript and approving it for publication was Feng Wei.

Subsequently, in actual antenna measurements, it is necessary to consider the aperture of each antenna (Antenna 1, Antenna 2). Therefore, the more appropriate DFF condition is shown in Equation (2). The minimum distance will be

$$R \geq \frac{2(D_1+D_2)^2}{\lambda} \tag{2}$$

where D_1 is the maximum size of Tx Antenna, D_2 is the maximum size of Rx Antenna, and λ is wavelength.

An example using the antennas shown in Figure 1 demonstrates the challenge of DFF measurements at 30 GHz. Antenna 1 is a 15 dBi horn antenna with an aperture of 20.2 mm x 19.5 mm. Antenna 2 is a 1024-element (32 × 32) patch array antenna with an aperture of 200 × 200 mm, and the array spacing is 0.65 λ. Suppose the longest part of each antenna is the aperture plane, D1 = 19.5 mm and D2 = 282.8 mm, and the DFF is calculated. In that case, it is necessary to provide a Test Range (TR) distance between antennas of at least approximately 18 m. The radiation measurement pattern shown in Figure 2 of the Rx antenna at Phi = 0 deg. demonstrates a challenge with DFF measurement techniques if this minimum TR distance is not respected when performing DFF measurements. The black line shows the far-field analysis values for Antenna 2 shown in Fig. 3, calculated using the finite element method (FEM). The blue dotted line shows the theoretical values calculated using the array factor (AF), and the red line shows the actual measurement results for Test Range (TR) = 2 m (≪18m). The theoretical and analytical values obtained using the AF and FEM show good agreement. However, suppose we focus on the actual measurement results, which do not satisfy the far-field TR condition of 18m. In that case, the directivity is not formed appropriately, and the null point exhibits a shoulder pattern, indicating the measurement is incorrect. Given that the maximum allowable TR distance between antennas of a typical radio wave anechoic chamber is around 3-5 m, this often presents a challenge. IFF measurement systems and techniques are increasingly used to address this problem and perform accurate antenna characterizations within the traditional footprint of an existing smaller chamber [4]. Compact Antenna Test Ranges (CATR) utilizing IFF techniques are becoming increasingly common for Beyond 5G/6G, satellite, and automotive radar antennas that use the millimeter wave band [5], [6], [7], [8].

However, these traditional CATR systems often use reflectors made using expensive, process intensive metal machining into curved surfaces. In addition, because reflectors are usually made of heavy metal, the supporting test structure must be large and robust. An alternative IFF measurement method, the Near-Field to Far-Field Transformation (NFFFT) technique, has been proposed to avoid the need for these expensive and heavy reflectors. The downside of this approach is that the large-scale positioner required to scan the near field must be carefully prepared and installed, and the measurement time is often long [9]. Traditional CATR systems (using metal reflectors) and NFFFT techniques have proven expensive and difficult to implement. The IFF CATR system, using a dielectric lens, was considered as a possible cost-effective alternative. The dielectric lens does not require the same high processing difficulty as metal reflectors and can be manufactured with a simpler support structure. It has been reported that the scattering waves at the edge of the dielectric lens worsen the Quiet Zone (QZ) characteristics of such a CATR system [10]. A method has been devised to reduce diffraction waves at the edge by forming a Serrated Structure (SS) at the edge of the lens [11]. This is a geometrically designed approach, not an electromagnetic field analysis approach. This paper concludes that using cosine-type SSs with lengths of 10-15λ and serration numbers of 32-64 can reduce diffraction waves significantly.

Therefore, we constructed a triangular SS considering prototyping, and through electromagnetic field analysis using FEM with Ansys HFSS, the diffraction wave was reduced at the edge with a length of approximately 4λ, a width of approximately 1λ, and 120 serrations [12]. This paper conducts parameter analysis of SS targeting the Ka band and examines a lens-type CATR system that can be manufactured inexpensively at 30 GHz. First, it describes the outline of the lens-type CATR, and then it optimizes the shape of the SS by performing a parameter study of the SS to reduce the diffraction wave at the edge of the lens. Next, the numerical analysis results are compared with the measured results of the plane wave characteristics at QZ. It also reports on the results of evaluating the radiation pattern of a 1024-element patch array antenna at 30 GHz using the lens-type CATR system.

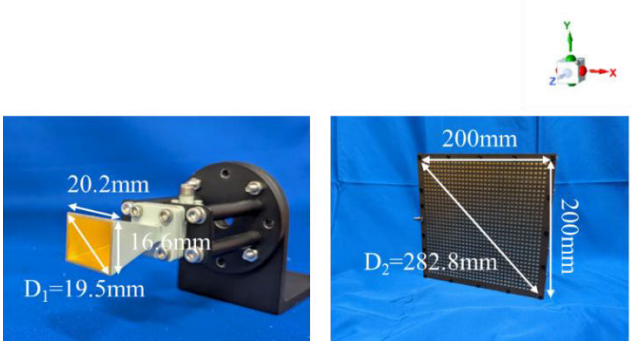

(a) Antenna 1 (b) Antenna 2

FIGURE 1. Tx and Rx antennas used in DFF calculations.

II. LENS-TYPE CATR SYSTEM

When considering a lens-type CATR system, as shown in Fig. 4, the refraction effect of the lens is used to collimate the spherical wave of the feeder antenna into a plane wave. The amplitude and phase conditions that satisfy the DFF requirements are achieved over a short distance. If the AUT (Antenna Under Test) is placed within the QZ, evaluating the antenna's radiation pattern in a short TR is possible. Furthermore, it is possible to expect an improvement in the dynamic range.

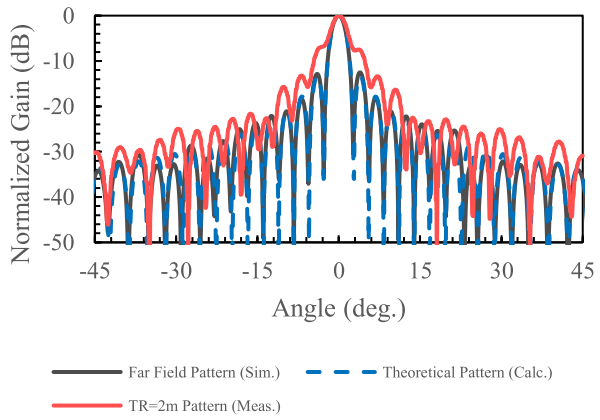

FIGURE 2. Rx antenna Phi = 0 deg. Plane radiation pattern (30GHz).

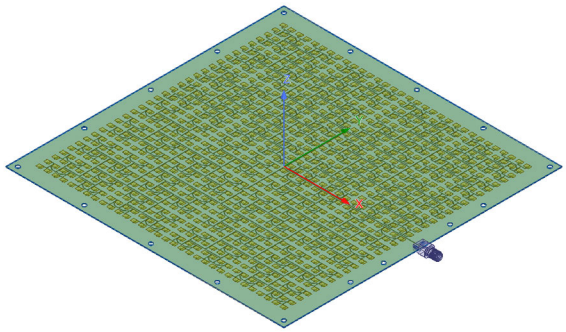

FIGURE 3. Antenna 2 simulation model.

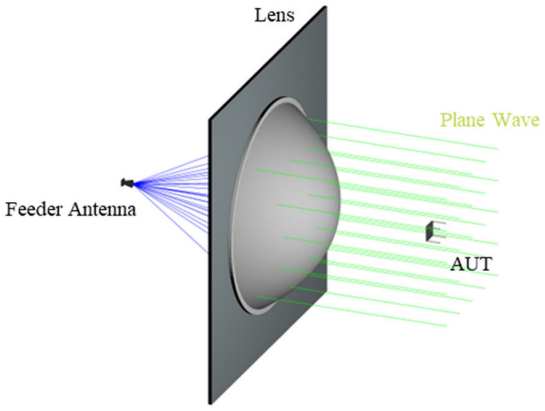

FIGURE 4. Lens-type CATR system.

As a general method for evaluating the characteristics of QZ plane waves, it is common to evaluate the amplitude and phase as shown in Fig. 5 [13]. The evaluation indicators are the ripple and taper levels of the curve obtained by the curve-fitting function within the QZ. In this study, the total variation within the QZ was evaluated as a measure of the planar wave characteristics in general. It is known that the planar wave characteristics of the CATR are within ±0.5 dB in amplitude and ±10 deg. in phase in terms of total variation [14]. This is a very high standard, but it is worth mentioning that the measurement accuracy can be maintained at 0.8 dB for CATR QZ Total Variation with Amplitude ≤ ±1.0 dB and Phase ≤ ±15 deg. [15]. Therefore, the evaluation indicators for the total variation of the plane wave characteristics of the CATR lens-type were set to Amplitude ≤ ±1.0 dB and Phase ≤ ±15 deg.

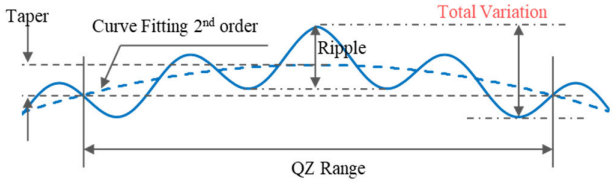

FIGURE 5. Plane wave ripple specifications.

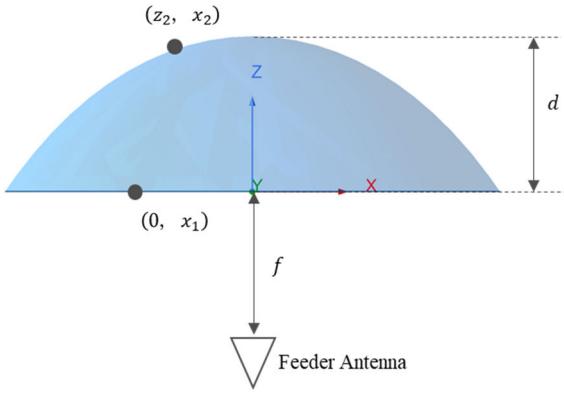

FIGURE 6. Lens design.

III. DESIGN OF LENS-TYPE CATR SYSTEM

As the lens of the lens-type CATR, the curvature was set to satisfy the Abbe sine condition, which has low aberration, as shown in Fig. 6 and Equation (3)-(4) [16], [17].

$$z_2 = \left\{ \frac{(n-1)\,d + f - \sqrt{f^2 + x_1^2}}{n - \left(1 - \left(\frac{x_1^2}{n^2\left(f^2 + x_1^2\right)}\right)\right)^{\frac{1}{2}}} \right\} * \left[1 - \frac{x_1^2}{n^2\left(f^2 + x_1^2\right)}\right]^{\frac{1}{2}} \tag{3}$$

$$x_2 = x_1 \left[1 + \frac{z_2}{\left[n^2\left(f^2 + x_1^2\right) - x_1^2\right]^{\frac{1}{2}}}\right] \tag{4}$$

The lens design was considered where n was the refractive index, f was the focal length, d was the lens's thickness, and λ was the wavelength.

I In this study, considering the prototype, we used polypropylene ($\varepsilon r = 2.25$, $\tan\delta = 0.003$, $n = 1.5$) as the material for the dielectric lens, as it is highly available and easy to process. It is assumed there will be fewer scattered waves at the lens boundary surface due to its low

relative permittivity. To obtain a QZ that is rotationally symmetric, it was thought that an antenna with a small difference between the E-plane and H-plane would be suitable, so the Conical Horn Antenna (CHA) shown in Fig. 7 was used. The port settings were made in the analysis so that the main polarization was parallel to the Y-axis. First, the analysis of the radiation pattern of the CHA was carried out. The radiation pattern of the CHA at 30 GHz is shown in Fig. 8. As a result, Gain = 16.0dBi, 3dB Beam Width (BW) was Phi = 0deg. Plane ±16.5 deg., Phi = 90deg. Plane ±13.7 deg., and 10dB BW was Phi = 0deg. Plane ±30.4 deg., Phi = 90deg. Plane ±24.3 deg. In addition, the antenna's phase center needed to be positioned at the lens's focal length. Therefore, this phase center of the antenna was analyzed. The phase characteristics were analyzed using the offset amount (Δz) in the Z-axis direction from the center of the aperture plane of the antenna. As a result, the phase pattern characteristics of the Phi = 0 deg. and 90 deg. planes at 30 GHz are shown in Figs. 9-10. The results were normalized with reference to the phase in the front direction, and the black, blue, and red lines show the phase patterns for $\Delta z = 0$, -2, and -4 mm, respectively. As a result, the phase planes for both the Phi = 0 deg. and 90 deg. planes were aligned within an approximate 10 dB BW range for $\Delta z = -2$ mm and were said to be the phase center. Therefore, the lens's focal length was to be positioned at -2 mm in the -Z axis direction from the aperture plane of this CHA. The lens design was such that the range where the phase planes are aligned was focused on the lens.

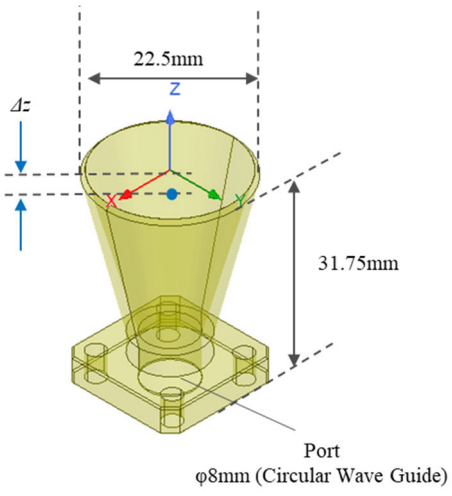

FIGURE 7. Feeder antenna for Lens-type CATR system.

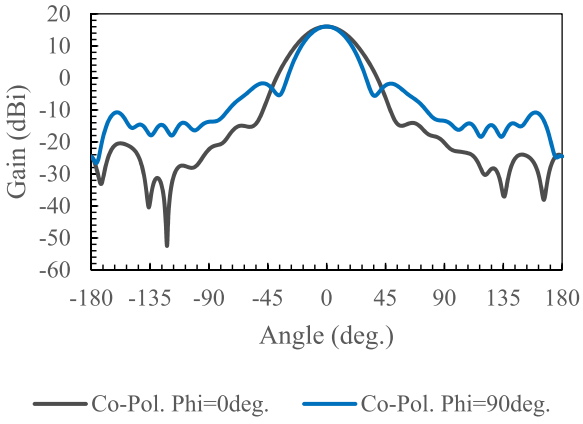

FIGURE 8. Radiation pattern of CHA (30 GHz).

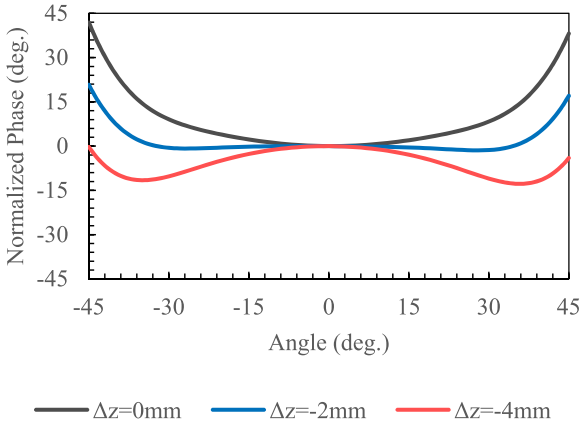

FIGURE 9. Phi = 0 deg. Plane phase pattern characteristics of CHA (30 GHz).

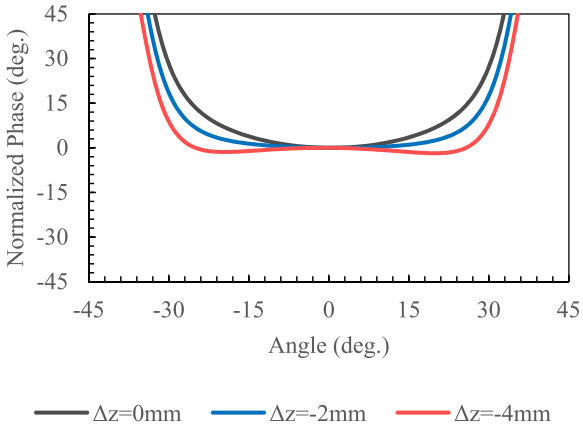

FIGURE 10. Phi = 90 deg. Plane phase pattern characteristics of CHA (30 GHz).

The lens-type CATR was designed as shown in Figs. 11-12, and the SS structure is shown in Fig. 13. The lens size was φ600 mm, and the focal length was 430 mm, so the focusing range was ±34.9 deg. to focus within 10 dB BW satisfactorily. The thickness of the lens was 200 mm. The metal plate that held the lens and the SS are defined as Perfect Electric Conductors (PEC). The thickness of the SS was 2 mm, and the thickness of the holding fixture was 10 mm. The SS was attached to the incident surface of the lens, and the shape was a triangle to facilitate manufacturing. The parameters considered were the triangle's tooth width (W), tooth length (L), and the number of SS.

An AZ turntable is used to measure the actual antenna radiation pattern. Therefore, considering the placement of the turntable, an observation line parallel to the X-axis was

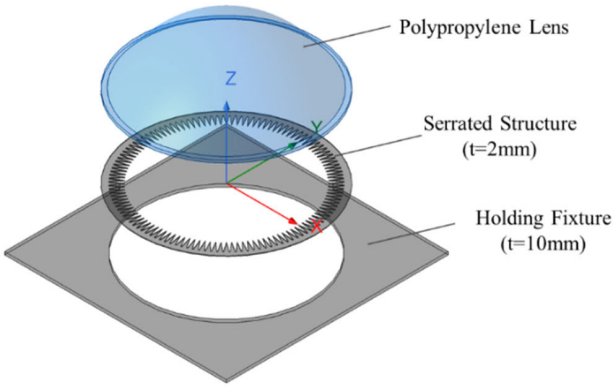

FIGURE 11. Exploded view.

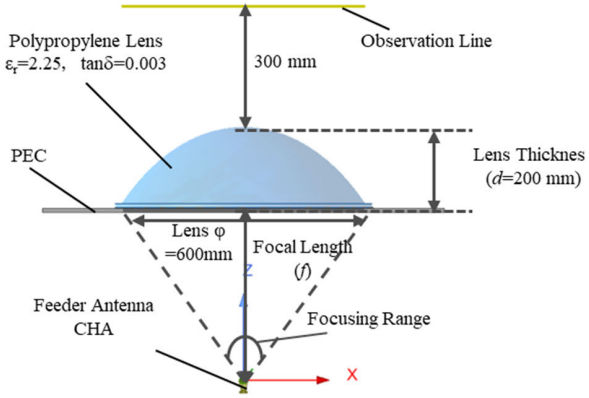

FIGURE 12. Designed lens type CATR system.

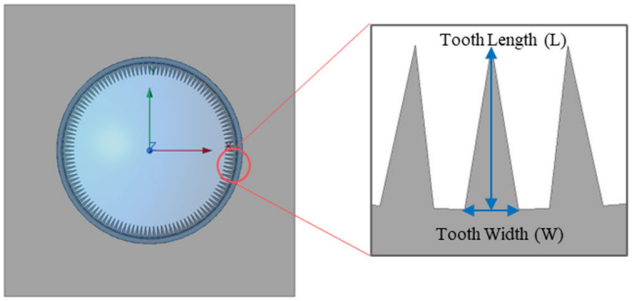

FIGURE 13. Serrated structure.

set at a position 300 mm from the apex of the lens, and an attempt was made to acquire the amplitude and phase of the Ey component, which was the main polarization. The QZ range was set to 1/3 of the lens size (= ±100 mm), and the plane wave characteristics were evaluated by evaluating the total variation.

IV. SIMULATION RESULTS

The initial parameters for the SS were set as Tooth_W = 13 mm (1.3λ) and Tooth_L = 40 mm (4λ). As shown in Fig. 14, the analysis was performed for the plane wave characteristics when the parameters were (a) Number of SS = 100 (3.6 deg. Spacing), (b) 120 (3 deg. Spacing), and (c) 144 (2.5 deg. Spacing). The plane wave characteristics at the 30GHz observation line are shown in Table 1 and Figs. 15-16. The black, blue, and red lines indicate SS = 100, 120, and 144, respectively.

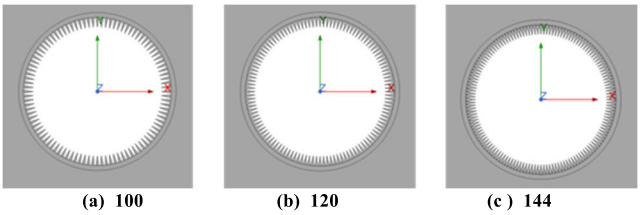

FIGURE 14. Number of serrated structure.

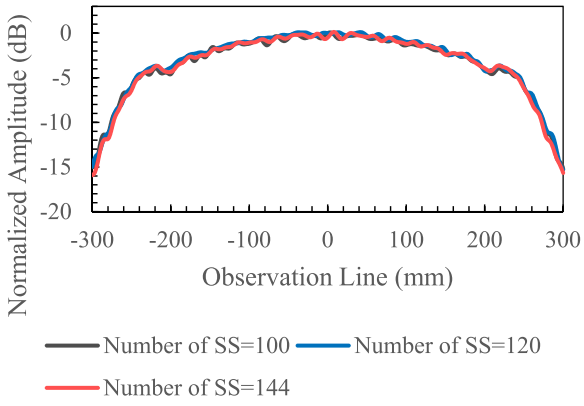

FIGURE 15. Amplitude characteristics (30 GHz). (Parameter is number of serrated structure).

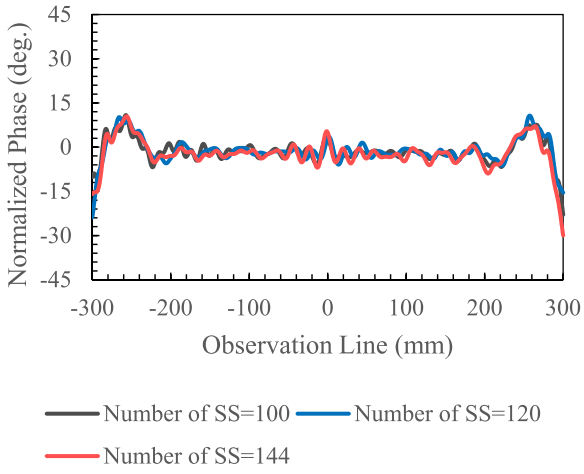

FIGURE 16. Phase characteristics (30 GHz). (Parameter is number of serrated structure).

Regarding the number of SS, the Total Variation of the amplitude was best when it was 120, at ±0.56 dB. The Total Variation of the phase was best when it was 100, at ±4.53 deg., but the characteristics are almost the same as when it was 120. In this case, the optimal value was set at 120, which gave a smooth characteristic for both phase and amplitude. After setting the number of SSs to 120, an evaluation was performed for Tooth_W and Tooth_L. The plane

TABLE 1. Plane wave characteristics (Parameter is number of serrated structure).

Evaluation Range =±100mm	Number of Serrated Structure		
	100	120	140
Amplitude	±0.73 dB	±0.56 dB	±0.67 dB
Phase	±4.53 deg.	±4.68 deg.	±6.16 deg.

wave characteristics of the amplitude and phase are shown in Table 2-3.

TABLE 2. Plane wave characteristics of amplitude (Parameter is Tooth_W and Tooth_L).

Evaluation Range =±100mm		Tooth_W		
		11 mm (1.1λ)	13 mm (1.3λ)	15 mm (1.5λ)
Tooth_L	37mm	±0.69 dB	±0.75 dB	±0.78 dB
	40mm	±0.64 dB	±0.56 dB	±0.69 dB
	43mm	±0.84 dB	±0.85 dB	±0.93 dB

TABLE 3. Plane wave characteristics of phase (Parameter is Tooth_W and Tooth_L).

Evaluation Range =±100mm		Tooth_W		
		11 mm (1.1λ)	13 mm (1.3λ)	15 mm (1.5λ)
Tooth_L	37mm (3.7λ)	±4.22 deg.	±4.31 deg.	±6.28 deg.
	40mm (4λ)	±3.44 deg.	±4.68 deg.	±5.71 deg.
	43mm (4.3λ)	±4.23 deg.	±4.56 deg.	±5.05 deg.

With the number of SS set to 120, the results of the parameter study for Tooth_W and Tooth_L showed that the optimum values were Tooth_W = 13 mm (1.3λ) and Tooth_L = 40 mm (4λ), which had the lowest amplitude difference and the best phase characteristics. The plane wave analysis results of the lens's amplitude and phase, w/ and w/o SS, are shown in Table 4 and Figs. 17-18. The black line is the analysis value for w/o SS, and the blue line is the value for w/ SS. In addition, the E-field distribution at 30 GHz is shown in Fig. 19 (w/o SS) and Fig. 20 (w/ SS). As a result, the plane wave characteristics w/ and w/o SS show improvement from ±1.74 dB to ±0.56 dB in amplitude and from ±9.39 deg. to ±4.68 deg. in phase. It was demonstrated, therefore, that the plane wave characteristics improve significantly with the incorporation of SS. If the E-field distribution is checked w/o SS, scattered waves can be seen in the direction of travel. In contrast, in the case of w/ SS, the distribution of standing waves increases at the lens's edge. It is thought that, as with the SS of the CATR reflector, the SS around the lens plays a role in scattering the diffraction waves generated by the edge [18]. Further, the interference of the diffracted wave is reduced, and the plane wave is improved for the progressing plane wave. In the design by numerical analysis, it is thought that it is possible to apply this to a CATR system because it is a plane wave characteristic of Amplitude ≤ ±1.0 dB and Phase ≤ ±15deg. that was determined as an evaluation indicator of QZ.

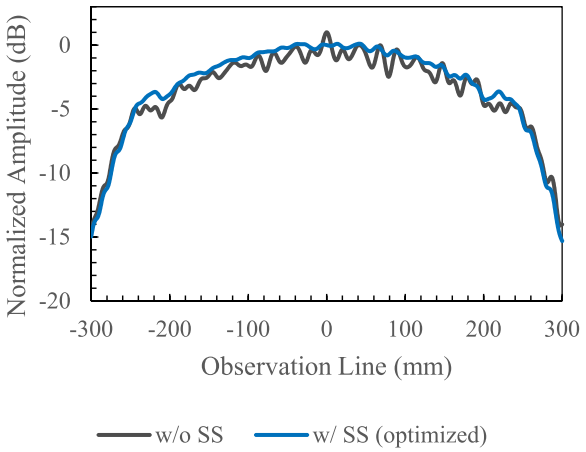

FIGURE 17. Plane wave characteristics of Amplitude in w/o SS vs w/ SS (30 GHz).

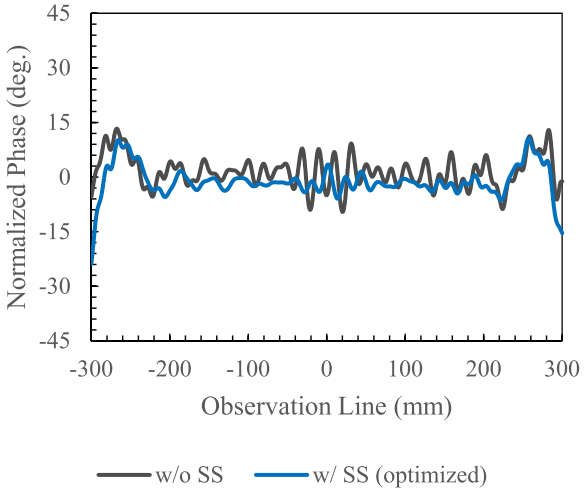

FIGURE 18. Plane wave characteristics of phase in w/o SS vs w/ SS (30 GHz).

V. TRIAL MANUFACTURE AND MEASUREMENT RESULTS

Prototypes of the analyzed dielectric lens and SS were made, and the validity of the analytical results was confirmed through empirical measurements. A Feeder Antenna was fabricated using the CHA derived using numerical analysis. As shown in Fig. 21, the amplitude and phase of the E-field were measured using the WR-28 Probe Antenna and a 1-axis scanner. The distances from the apex of the lens to the probe

TABLE 4. Plane wave characteristics in w/o SS vs w/ SS.

Evaluation Range =±100mm	w/o SS	w/ SS (optimized)
Amplitude	±1.74 dB	±0.56 dB
Phase	±9.39 deg.	±4.68 deg.

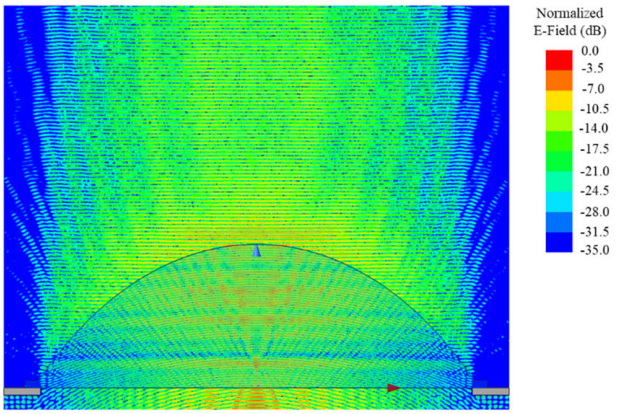

FIGURE 19. E-field strength distribution map of w/o SS (30 GHz).

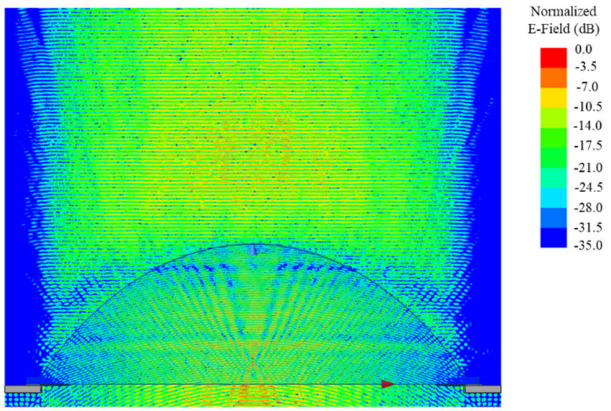

FIGURE 20. E-field strength distribution map of w/ SS (30 GHz).

antenna was 300 mm. The scanning range of the scanner was ±250 mm, and the amplitude and phase were measured using a vector network analyzer (VNA) at 1 mm steps. The plane wave's characteristics were measured in the cases of w/o SS(a) and w/ SS(b), as shown in Figure 22. The validity of the results was confirmed by comparing them with the results of the numerical analysis. The measured results for the amplitude and phase characteristics of the plane wave at 30 GHz are shown in Figs. 23-24. The black line is w/o SS, the blue line is w/ SS, the solid line is the measured value, and the dotted line is the analytical value. Table 5 summarizes the comparison between the numerical analysis and the measured results for the total variation in the QZ range of ±100 mm.

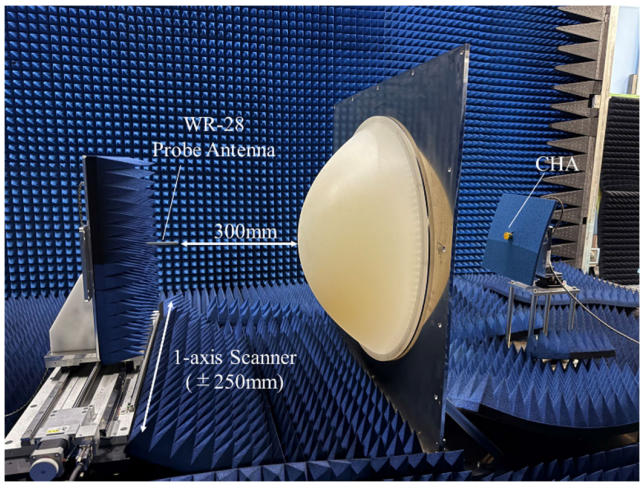

FIGURE 21. The manufactured polypropylene lens, CHA and measurement of plane wave characteristics.

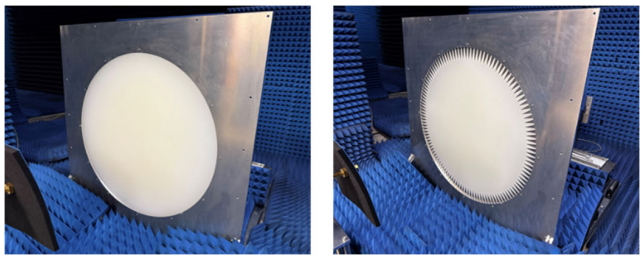

(a) w/o SS (b) w/ SS

FIGURE 22. The manufactured serrated structure.

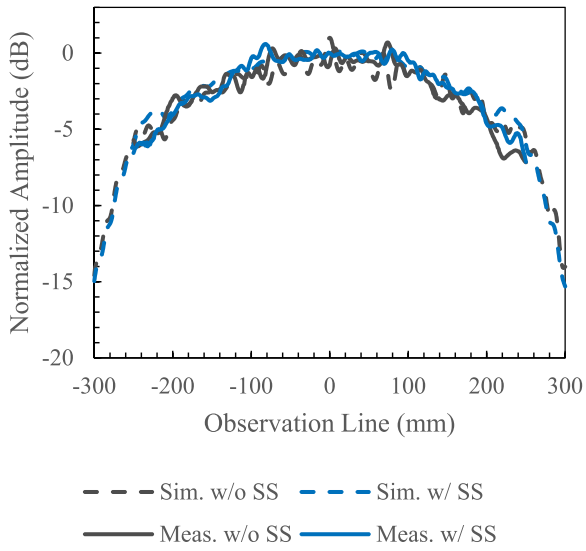

FIGURE 23. Measured amplitude of plane wave characteristics in w/ SS vs w/o SS (30 GHz).

As a result, it was confirmed that the ripple was reduced by setting the SS using the measurement results. For the plane wave characteristics within the QZ evaluation range of ±100 mm, the amplitude improved from ±1.19 dB to ±0.65 dB, and the phase improved from ±8.08 deg.

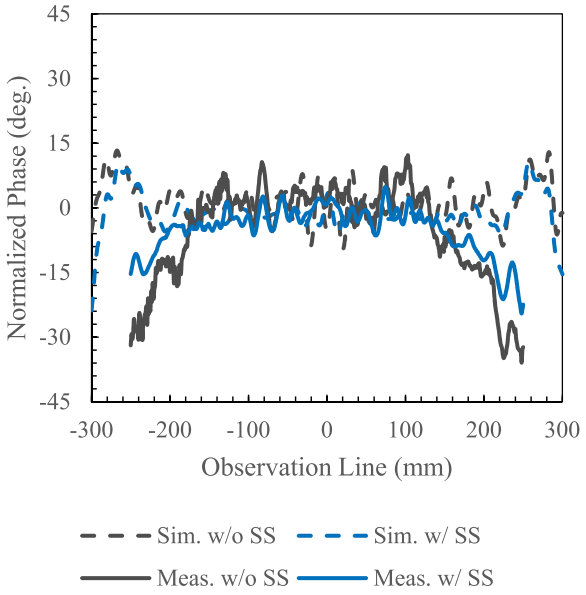

FIGURE 24. Measured phase of plane wave characteristics in w/ SS vs w/o SS (30 GHz).

TABLE 5. Measured plane wave characteristics in w/o SS vs w/ SS.

	Evaluation Range =±100mm	Amplitude	Phase
w/o SS	Sim.	±1.74 dB	±9.29 deg.
	Meas.	±1.19 dB	±8.08 deg.
w/ SS	Sim.	±0.56 dB	±4.68 deg.
	Meas.	±0.65 dB	±5.59 deg.

to ±5.59 deg. In addition, the numerical analysis results and the measured characteristics of both the amplitude and phase were generally equivalent, and the validity of the numerical analysis model was confirmed. Therefore, it was confirmed that the SS contributed to improving the characteristics of the plane wave by scattering the diffraction wave at the edge of the lens using the SS. Measurements showed the plane wave characteristics of Amplitude $\leq \pm 1.0$ dB and Phase $\leq \pm 15$ deg., which were determined as the evaluation indicators for QZ, making it possible to use an SS in a CATR system.

VI. ANTENNA RADIATION PATTERN EVALUATION

In the previous chapter, it was confirmed that the lens-type CATR system satisfied the evaluation indicators Amplitude $\leq \pm 1.0$ dB and Phase $\leq \pm 15$ deg. for the QZ characteristics within ±100 mm at a distance of 300 mm from the top of the lens, which is the position where the AUT was placed. The system's validity was confirmed by measuring the AUT radiation pattern of a 1024-element patch array antenna (200 × 200mm) at 30 GHz. The DFF condition for the AUT was 18 m or more. Fig. 25 shows the measurement at a short distance using the CATR. The AUT was placed on the AZ-positioner so that the center of the AUT was directly opposite the top of the lens at 300 mm. The size of the AUT was 200 × 200 mm, so it fit within the QZ range of the lens. The rotation stage was controlled in ±45 deg. (0.1 deg. step), and the radiation pattern was obtained by measuring the amplitude characteristics at each angle. Then, the orientation of the AUT was changed to attempt to measure the H-Plane (Phi = 0 deg. Plane) and E-Plane (Phi = 90 deg. Plane).

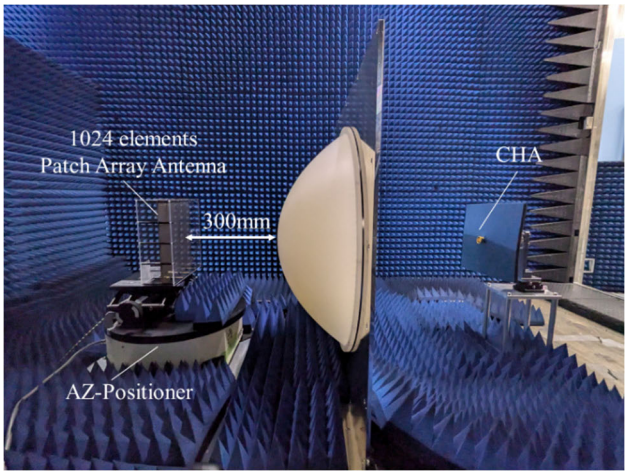

FIGURE 25. 1024 elements patch array antenna radiation pattern evaluation.

The radiation patterns of the 1024-element patch array antenna at 30 GHz, measured at Phi = 0deg. and Phi = 90deg., are shown in Fig. 26 and Fig. 27. The black line shows values from the EM analysis, and the blue line shows the radiation pattern measured using the lens-type CATR. As an evaluation of the match between the radiation patterns, the 3dB Beam Width (BW) and the Side Lobe Level (SLL) of the 1st Side Lobe were evaluated. The results are summarized in Table 6.

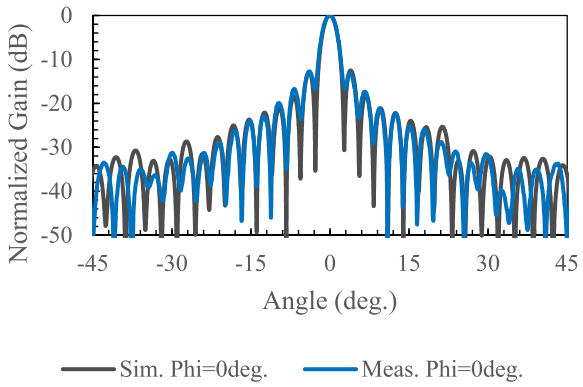

FIGURE 26. Phi = 0deg. Plane AUT radiation pattern (30GHz).

These results show that although the 18 m DFF range distance was not met, the far-field results of the measured radiation pattern and the analytical value at the 300 mm position agreed when using the lens-type CATR. When evaluating the radiation patterns of the measured and analytical values

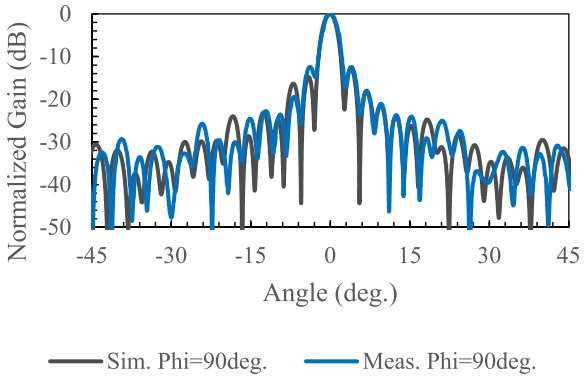

FIGURE 27. Phi = 90deg. Plane AUT radiation pattern (30GHz).

TABLE 6. AUT radiation pattern evaluation.

Evaluation Range =±100mm		3dB BW	SLL
Phi=0 deg. Plane	Meas.	2.5 deg.	12.4 dB
	Sim.	2.4 deg.	12.8 dB
Phi=90 deg. Plane	Meas.	2.5 deg.	12.4 dB
	Sim.	2.5 deg.	12.7 dB

of the AUT, the 3 dB BW and the SLL showed a good match within approximately 0.4 dB. It might be tempting to assume this was due to some measurement error and the in-plane variation of the relative permittivity of the substrate. However, the fact that the angle of the 1st Side Lobe was consistent at ±4 deg., and the angles of each null point were also consistent, suggested the measurement was carried out accurately.

VII. CONCLUSION

For 5G high-gain antennas in the Ka-band, lens-type CATR systems were considered for evaluating antennas with apertures that are sufficiently larger relative to their wavelength. Conventionally, reflector-type CATR systems have been successfully used to reduce the size of test ranges. However, due to the expense of metal processing, these reflectors have proven to be expensive to manufacture accurately. It was thought that a low-cost CATR system could be realized using a dielectric lens to address these economic challenges. The degradation of the planar wave characteristics of these lower-cost dielectric lenses due to diffraction waves at the lens edge proved problematic. Therefore, SS was introduced around the lens's incidence surface. Analysis and measurement verified that the scattering of the incident path at the lens's edge by this SS reduced the effect of diffraction waves.

First, the plane wave characteristics of the lens-type CATR system QA were analyzed using EM analysis. As a result, it was confirmed that the quality of the plane wave was improved by setting the optimized SS, with the amplitude changing from ±1.74 dB to ±0.56 dB and the phase changing from ±9.39 deg. to ±4.68 deg. Next, the SS and lens were manufactured, and the plane wave characteristics were measured. It was confirmed that the amplitude was ±1.19 dB to ±0.65 dB and the phase was ±8.08 deg. to ±5.59 deg., which matched the numerical analysis. It was further verified that the plane wave characteristics of Amplitude ≤ ±1.0 dB and Phase ≤ ±15 deg., which were determined as the evaluation indicators for QZ, were achieved.

The lens-type CATR was then used to evaluate a 30 GHz 1024-element patch array antenna. The results showed a good match between the analytically predicted and measured radiation patterns. Further, it was confirmed that the lens-type CATR studied here could be applied as a far-field measurement system. Thus, when measuring an antenna with an aperture that would not usually satisfy the 18 m DFF condition, it was possible to evaluate the antenna radiation pattern in a compact range of only 300 mm using the CATR with SS.

As future work, it is necessary to analyze and measure the frequency characteristics of the plane wave over a wide bandwidth. In addition, it is necessary to evaluate the sensitive analysis of manufacturing errors. Also, the radiation patterns measured using the reflector-type CATR will be compared with those measured using the DFF. Furthermore, it is essential to investigate the accuracy of the measurements further.

REFERENCES

[1] A. Ghosh, A. Maeder, M. Baker, and D. Chandramouli, "5G evolution: A view on 5G cellular technology beyond 3GPP release 15," *IEEE Access*, vol. 7, pp. 127639–127651, 2019.

[2] S. Han, C. Lin I, C. Rowell, Z. Xu, S. Wang, and Z. Pan, "Large scale antenna system with hybrid digital and analog beamforming structure," in *Proc. IEEE Int. Conf. Commun. Workshops (ICC)*, Sydney, NSW, Australia, Jun. 2014, pp. 842–847.

[3] V. J. Vokurka, "Advanced antenna measurements," in *Proc. 14th Eur. Microw. Conf.*, Liege, Belgium, Oct. 1984, pp. 60–70.

[4] C. Parini, A. D. Olver, P. McNair, and C. J. Prior, "The design, construction and use of a millimetrewave compact antenna test range," in *Proc. 6th Int. Conf. Antennas Propag.*, Coventry, U.K., Apr. 1989, pp. 345–350.

[5] C. -L. Liao, Y. -H. Lin, I. Lin, and C. -F. Yang, "A plane-wave scene emulation range for OTA performance evaluation of radio units for B5G/6G wireless communication systems," in *Proc. Antenna Meas. Techn. Assoc. Symp. (AMTA)*, Cincinnati, OH, USA, 2024, pp. 1–6.

[6] S.-H. Park, Y.-N. Kim, H.-Y. Kim, T.-S. Moon, and J.-H. Park, "Active performance verification of 28 GHz 5G beam-forimg antenna module using CATR chamber," in *Proc. Int. Symp. Antennas Propag. (ISAP)*, Incheon, South Korea, Nov. 2024, pp. 1–2.

[7] R. Liu, I. Lin, J. Liang, and R. Lin, "A new compact test range for satellite antenna measurements," in *Proc. Int. Symp. Antennas Propag. Conf.*, Kaohsiung, Taiwan, Dec. 2014, pp. 1–2.

[8] R.-C. Liu, C.-H. Li, T.-H. Lee, and Y.-C. Kan, "Automotive radar precision calibration with compact antenna test range," in *Proc. IEEE Int. Conf. Consum. Electronics-Taiwan (ICCE-TW)*, Penghu, Taiwan, Sep. 2021, pp. 1–2.

[9] R. Cariou and P. Massaloux, "Near field far field transformation: Calculation and application," in *Proc. IEEE Int. Symp. Antennas Propag.*, Chicago, IL, USA, Jul. 2012, pp. 1–2.

[10] M. Multari, J. Lanteri, J. L. Le Sonn, L. Brochier, C. Pichot, C. Migliaccio, J. L. Desvilles, and P. Feil, "77 GHz stepped lens with sectorial radiation pattern as primary feed of a lens based CATR," *IEEE Trans. Antennas Propag.*, vol. 58, no. 1, pp. 207–211, Jan. 2010.

[11] T. Hirvonen, J. Tuovinen, and A. V. Räisänen, "Lens-type compact antenna test range at MM-waves," in *Proc. 21st Eur. Microw. Conf.*, Stuttgart, Germany, Sep. 1991, pp. 1079–1083.

[12] G. Hattori, S. Ema, Y. Horie, and T. Maeyama, "Plane wave characteristics of a dielectric lens antenna with serrated structure for CATR systems," in *Proc. Int. Symp. Antennas Propag. (ISAP)*, Incheon, South Korea, Nov. 2024, pp. 1–2.
[13] S. F. Gregson and C. G. Parini, "Examination of the effect of common CATR quiet zone specifications on antenna pattern measurement uncertainties," in *Proc. Loughborough Antennas Propag. Conf. (LAPC)*, Loughborough, Nov. 2017, pp. 1–5.
[14] L. Xiao, Y. Xie, and P. Wu, "An accurate analytical method to determine the range of quiet zone in compact antenna test range," *IEEE Trans. Instrum. Meas.*, vol. 73, pp. 1–8, 2024.
[15] E. B. Joy and R. E. Wilson, "Low sidelobe reflectors for compact ranges," in *Proc. 11th ESTEC Antenna Workshop Antenna Meas.*, Gothenburg, 1988, pp. 95–103.
[16] J. Volakis, *Antenna Engineering Handbook*, 4th ed., New York, NY, USA: McGraw-Hill, 2007, pp. 650–653.
[17] T. Okura, H. Tsuji, R. Miura, T. Kan, T. Matsuda, M. Toyoshima, J. Suzuki, and Y. Kishiyama, "Prototype evaluation of the 38 GHz-band lens antenna for high altitude platform station (HAPS) ground station system," in *Proc. 24th Int. Symp. Wireless Pers. Multimedia Commun. (WPMC)*, Okayama, Japan, Dec. 2021, pp. 1–5.
[18] Y. Jiang, C. Mo, W. Chen, and D. Kong, "Research on serrations of reflector used in CATR," in *Proc. Photon. Electromagn. Res. Symp. Fall (PIERS-Fall)*, Xiamen, China, Dec. 2019, pp. 1665–1669.

GENMA HATTORI (Member, IEEE) was born in Saitama, Japan, in June 1993. He received the B.E., M.E., and Ph.D. degrees in engineering from Takushoku University, Tokyo, Japan, in 2016, 2018, and April 2024, respectively. He was with Buffalo Inc., from April 2018 to February 2020. He was involved in the development of wireless LAN routers. He has been with Microwave Factory Company Ltd., since March 2020. He is engaged in the development of antennas and measurement systems for beyond 5G/6G.

SOU EMA was born in Aichi, Japan, in November 1998. He received the B.S. degree in science and engineering from Yokohama National University, Yokohama, Japan, in 2023. He has been with Microwave Factory Company Ltd., since April 2023. He is currently engaged in the development of antennas and measurement systems for beyond 5G/6G.

YUTA HORIE was born in Tokyo, Japan, in December 1979. He received the B.E. degree in engineering from Toyo University, in 2002, Saitama, Japan. He was with Nihon Dengyo Kosaku Company Ltd., from April 2002 to August 2017, and was involved in the research and development of antennas and RF circuits. He has been with Microwave Factory Company Ltd., since September 2017, and is involved in the research and development of RF equipment, such as automotive radar inspection equipment.

TOSHIYUKI MAEYAMA (Member, IEEE) was born in Tokyo, Japan, in 1967. He received the B.E., M.E., and Ph.D. degrees from Takushoku University, in 1991, 1993, and 1996, respectively. He joined DDI Tokyo Pocket Telephone Company, in 1996, and was engaged in research on antennas and propagation, wireless communication systems, and wireless body area networks. In 1996, he joined the Kyocera DDI Future Communications Laboratory. In 1998, he joined DDI Corporation (now KDDI Corporation). In 2001, he joined KDDI Research and Development Laboratories. In 2008, he became an Associate Professor at the Faculty of Engineering, Takushoku University. In 2017, he became a Professor at Takushoku University. Currently, he is the Vice President of Takushoku University. He is engaged in research on antennas, propagation, and wireless mobile communications, and the IoT. He received the 16th Radio Achievement Award.

CRFE

CORNES RF ENGINEERING

About Cornes RF Engineering

Microwave Factory Company (MWF) and E&C Engineering (ECE) are divisions of Cornes Technologies Limited headquartered in Tokyo, Japan. Together they make up Cornes RF Engineering (CRFE).

CRFE is committed to providing the industry with ADAS (radar, LiDAR, camera sensor), ESD, and antenna test system components (positioners, RF absorbing material, automated software and chambers) at price points that enable their broad utilization.

Cornes Technologies USA is the US distributor of CRFE, Microwave Factory and E&C Engineering products.

CORNES Technologies USA

www.cornestech.com
info@cornestech.com
780 Montague Expy., Ste. 506
San Jose, CA 95131
408-520-4550

Microwave Factory Company